

# 15

## Modeling Electric Field Distribution *In Vivo*

---

Nataša Pavšelj  
Anže Županič  
Damijan Miklavčič

15.1	Introduction .....	299
15.2	Electromagnetic Field Theory.....	300
	Maxwell's Equations • Constitutive Relations • Boundary Conditions • Electric Field Calculations for Electroporation	
15.3	Biological Tissues.....	302
	Biological Tissues in Electric Field • Biological Tissue in DC Electric Field • Some Biological Tissue Properties Important in the Applied Use of Electroporation	
15.4	Modeling .....	309
	Building a Geometry • Setting the Physics of the Model • Interpretation of Results • Model Verification and Validation	
15.5	Treatment Planning.....	315
15.6	Summary.....	318
	Acknowledgments.....	318
	References.....	318

### 15.1 Introduction

---

The application of electric pulses to cells, either in suspension or tissue, causes the electroporation of the cell membrane, increasing its permeability and making it possible for larger molecules that otherwise cannot cross the membrane, such as drug molecules or DNA, to enter the cell. If the pulse is of adequate amplitude, the electric field and consequently the induced transmembrane voltage are high enough to cause cell membrane permeabilization. For any given cell, the induced transmembrane voltage is proportional to the electric field; more precisely, it is proportional to the local electric field in which the cell is placed. More details on induced transmembrane voltage and electroporation on the cell level are given in Chapter 3, titled “Induced transmembrane voltage—Theory, modeling, and experiments” by Kotnik and Pucihar. In this chapter, the focus is on the electroporation on a tissue level, more specifically on how the electric field is distributed in different electrode-tissue setups in the applied use of electroporation.

Numerous experiments, both *in vitro* and *in vivo*, have to be performed before a biomedical application is put to practical use in the clinical environment. As a complementary work to *in vivo* experimenting, analytical and numerical models can be used to represent, as realistically as possible, real biological phenomena. In this way, we can better understand some of the processes involved and analyze and explain the experimental results. Different electrical parameters can be evaluated in advance, such as pulse amplitude, duration, and number of pulses. All of that can help us plan new protocols, design electroporation devices, facilitate the design of electrodes and their placement with respect to target tissue, and plan new experiments and treatments (Šemrov and Miklavčič 1998, Brandisky and Daskalov 1999,

Miklavčič et al. 2000, Dev et al. 2003, Miklavčič et al. 2006a, Šel et al. 2007, Čorović et al. 2008b, Županić et al. 2008). Of course, models have to be validated by experiments and, if necessary, improved. Experimenting with such models is easier and sometimes the only possible or ethically acceptable alternative to experimenting on real biological systems. Both experimental work and numerical modeling combined give us valuable information and help us to understand the underlying mechanisms of the process(es) we are aiming to describe.

As a simple definition, a mathematical model is a representation of the chosen essential aspects of a real system (may it be a living, engineering, or social system), described by a set of variables and a set of equations that establish relationships between the variables. Mathematical models represent an important tool in the study of the effects of the electromagnetic fields and accompanying coupled phenomena on cells, tissues, and organs (Fear and Stuchly 1998, Debruin and Krassowska 1999a,b, Miklavčič et al. 2000, Šel et al. 2005, Pavšelj and Miklavčič 2008a). These biological systems are often geometrically highly intricate, so analytical methods are, in most cases, entirely replaced by numerical methods. In continuation, we provide the basics of electromagnetic field theory, describe the characteristics of biological tissues, explain the basic steps in constructing numerical models of tissue electroporation, and give some reference to numerical modeling-based treatment planning.

## 15.2 Electromagnetic Field Theory

---

### 15.2.1 Maxwell's Equations

In 1865, Maxwell had put forward a set of equations that describe the properties of the macroscopic electric and magnetic fields and relate them to their sources: Ampere's law (Equation 15.1), Faraday's law of induction (Equation 15.2), Gauss's laws (Equation 15.3), Gauss's law for magnetism (Equation 15.4), and the continuity equation (Equation 15.5)

$$\nabla \times \vec{B} = \mu_0 \vec{J} + \mu_0 \epsilon_0 \frac{\partial \vec{E}}{\partial t} \quad (15.1)$$

$$\nabla \times \vec{E} = -\frac{\partial \vec{B}}{\partial t} \quad (15.2)$$

$$\nabla \cdot \vec{E} = \frac{\rho}{\epsilon_0} \quad (15.3)$$

$$\nabla \cdot \vec{B} = 0 \quad (15.4)$$

$$\nabla \cdot \vec{J} = -\frac{\partial \rho}{\partial t} \quad (15.5)$$

where

$\vec{B}$  is the magnetic flux density

$\vec{J}$  is the total current density

$\vec{E}$  is the electric field

$\rho$  is the electric charge

$\mu_0$  is the permeability of free space

$\epsilon_0$  is the permittivity of free space

When complemented by the constitutive relations pertaining to the media under consideration and by their relevant boundary conditions, these equations are suitable for initiating the numerical or analytical

solution of a given problem. Today, numerical calculations of the distribution of macroscopic electric and magnetic fields are usually performed using different sets of equations (Equations 15.6 and 15.7), usually derived from Maxwell's equations and the definitions of the electric potential  $V$  (Equation 15.8) and the magnetic vector potential  $A$  (Equation 15.9):

$$\nabla^2 V + \frac{\partial}{\partial t} (\nabla \cdot \vec{A}) = -\frac{\rho}{\epsilon_0} \quad (15.6)$$

$$\left( \nabla^2 \vec{A} - \frac{1}{c^2} \frac{\partial^2 \vec{A}}{\partial t^2} \right) - \nabla \left( \nabla \cdot \vec{A} + \frac{1}{c^2} \frac{\partial V}{\partial t} \right) = -\mu_0 \vec{J} \quad (15.7)$$

$$\vec{E} = -\nabla V - \frac{\partial \vec{A}}{\partial t} \quad (15.8)$$

$$\vec{B} = \nabla \times \vec{A} \quad (15.9)$$

By working with potentials instead of fields, the number of degrees of freedom of the calculations is reduced, as  $V$  and  $A$  only have four components to be solved for instead of six for  $E$  and  $B$ .

### 15.2.2 Constitutive Relations

When electromagnetic fields are applied to matter, the polarization and magnetization of bound charges and currents take place. By considering the constitutive relations for dielectric and magnetic materials (Equations 15.10 and 15.11)

$$\vec{D} = \epsilon \vec{E} \quad (15.10)$$

$$\vec{B} = \mu \vec{H} \quad (15.11)$$

where

$D$  is the electric flux density

$H$  is the magnetic field intensity

$\epsilon$  is the permittivity

$\mu$  is the permeability

A new set of Maxwell's equation is derived (Equations 15.12 through 15.15)

$$\nabla \times \left( \frac{\vec{B}}{\mu} \right) = \vec{J}_f + \epsilon \frac{\partial \vec{E}}{\partial t} \quad (15.12)$$

$$\nabla \times \vec{E} = -\frac{\partial \vec{B}}{\partial t} \quad (15.13)$$

$$\nabla \cdot (\epsilon \vec{E}) = \rho_f \quad (15.14)$$

$$\nabla \cdot \vec{B} = 0 \quad (15.15)$$

where

$J_f$  is the free current

$\rho_f$  is the free charge

It is worth noting that neither  $\epsilon$  nor  $\mu$  are necessarily constants, rather they are functions that can depend on position, field strength, field direction, or frequency. The same is true for the electrical conductivity that describes the relation between electric fields and electric currents in matter—Ohm's law (Equation 15.16). We focus on the physical properties of biological materials relevant to electroporation in Section 15.3 of this chapter.

$$\vec{J} = \sigma \vec{E} \quad (15.16)$$

### 15.2.3 Boundary Conditions

Since calculation of electromagnetic fields is usually limited to a finite region of space and time, it is necessary to use boundary and initial conditions. In modeling electric fields in biological tissues, the fields are introduced into the region of interest via Dirichlet (Equation 15.17) and Neumann (Equation 15.18) boundary conditions:

$$V = V_0 \quad (15.17)$$

$$\frac{\partial V}{\partial n} = q_0 \quad (15.18)$$

While the Dirichlet boundary condition specifies the value that the solution (in our case electric potential) takes on the boundary, the Neumann boundary condition specifies the value of the derivative of the solution on the boundary.

### 15.2.4 Electric Field Calculations for Electroporation

According to the theory of electroporation (see Chapter 3 by Kotnik and Pucihar in this book), when a cell is exposed to an external electric field, a transmembrane potential proportional to the field is induced on the cell plasma membrane. Since the magnitude of the induced transmembrane potential is related to the level of membrane permeabilization, bulk electroporation can be related to the local electric field distribution.

Most often, the electric fields used for electroporation are delivered in the form of unipolar rectangular electric pulses. These pulses are much longer than the membrane charging time; therefore, the induced transmembrane voltage reaches its final value long before the end of the pulse. This means that the electric field distribution can be modeled in its steady-state, disregarding the transients that occur during the pulse rise time. In practice, this means that equations used to calculate the local electric field distribution in electroporation modeling become much simpler. Note that the equations are still nonlinear, the nonlinearity being hidden in the material properties. The equations are reduced to the Laplace steady-state equation (Equation 15.19), which can be derived from Equations 15.5, 15.8, and 15.16 by taking into account that all time derivatives are equal to zero.

$$\nabla \cdot (\sigma \nabla V) = 0 \quad (15.19)$$

---

## 15.3 Biological Tissues

Biological tissues perform different physiological functions, which are reflected in a number of specific characteristics that have to be considered when representing them in a model at both the cellular and higher organizational level. These differences are also clearly reflected in highly different bulk properties of biological materials (Gabriel et al. 1996a,b, Miklavčič et al. 2006b). They define the current densities

and pathways that result from an applied electric stimulus and are thus very important in the analysis of a wide range of biomedical applications used for diagnosis and treatment. Biological tissues are, in general, inhomogeneous and nonlinear.

### 15.3.1 Biological Tissues in Electric Field

The electrical properties of any material, including biological tissue, can be broadly separated into two categories: conducting and insulating. In a conductor, the electric charges move freely in response to the applied electric field whereas in an insulator (dielectric) the charges are fixed and are not free to move. A more detailed discussion of the fundamental processes underlying the electrical properties of tissue can be found in Foster and Schwan (1989).

If a conductor is placed in an electric field, charges will move within the conductor until the interior field is zero. In the case of an insulator, there are no free charges; therefore, the net migration of charge does not occur. In polar materials, however, the positive and negative charge centers in the molecules do not coincide, which causes an electric dipole moment,  $p$ . An applied field,  $E_0$ , tends to orient the dipoles and produces a field inside the dielectric,  $E_p$ , which opposes the applied field. This process is called polarization. Most materials contain a combination of orientable dipoles and relatively free charges so that the electric field is reduced in any material. The net field inside the material,  $E$ , is then

$$\vec{E} = \vec{E}_0 - \vec{E}_p \quad (15.20)$$

The net field is lowered by a significant amount relative to the applied field if the material is an insulator and is essentially zero for a good conductor. This reduction is characterized by a factor  $\epsilon_r$ , which is called the relative permittivity or dielectric constant, according to

$$\vec{E} = \frac{\vec{E}_0}{\epsilon_r} \quad (15.21)$$

In practice, most materials, including biological tissue, actually display some characteristics of both insulators and conductors because they contain dipoles as well as free charges that can move, but in a restricted manner. For materials that are heterogeneous in structure, charges may become trapped at interfaces. Because positive and negative ions move in opposite directions in the applied field, internal charge separations can then result within the material, producing an effective internal polarization that acts like a very large dipole.

On the macroscopic level, we describe the material as having a permittivity,  $\epsilon$ , and a conductivity,  $\sigma$ . The permittivity characterizes the material's ability to trap or store charge or to rotate molecular dipoles whereas the conductivity describes its ability to transport charge (Grimnes and Martinsen 2000):

$$\epsilon = \epsilon_r \epsilon_0 \quad (15.22)$$

Consider a sample of material that has a thickness,  $d$ , and cross-sectional area,  $A$ . If the material is an insulator, then we treat the sample as a capacitor with a capacitance of

$$C = \epsilon \cdot \frac{A}{d} \quad (15.23)$$

If it is a conductor, then we treat it as a conductor with a conductance of

$$G = \sigma \cdot \frac{A}{d} \quad (15.24)$$

If a constant (direct current, DC) voltage  $V$  is applied across this parallel combination, then a conduction current  $I_C = GV$  will flow and an amount of charge  $Q = CV$  will be stored.

Suppose, instead, we apply an alternating (alternating current, AC) voltage:

$$V(t) = V_0 \cos(\omega t) \quad (15.25)$$

where

$V_0$  is the amplitude of the voltage

$\omega = 2\pi f$ , where  $f$  is the frequency of the applied signal

The charge on the capacitor plates is now changing with frequency  $f$ . This change is associated with a flow of charge or current in the circuit. We characterize this flow as a displacement current:

$$I_d = \frac{dQ}{dt} = -\omega C V_0 \sin(\omega t) \quad (15.26)$$

The total current flowing through the material is the sum of the conductive and displacement currents that are separated in phase by  $90^\circ$ . This phase difference can be expressed as

$$V(t) = V_0 e^{i\omega t} \quad \text{where } i = \sqrt{(-1)} \quad (15.27)$$

taking its real part for physical significance. The total current is  $I = I_c + I_d$  ( $I_c$  being the conductive and  $I_d$  being the displacement current), hence

$$I = GV + C \cdot \frac{dV}{dt} = (\sigma + i\omega\epsilon)A \cdot \frac{V}{d} \quad (15.28)$$

The actual material, then, can be characterized as having an admittance,  $Y^*$ , given by

$$Y^* = G + i\omega C = \left( \frac{A}{d} \right) (\sigma + i\omega\epsilon) \quad (15.29)$$

where  $*$  indicates a complex-valued quantity. In terms of material properties, we define a corresponding, complex-valued conductivity or admittivity as

$$\sigma^* = (\sigma + i\omega\epsilon) \quad (15.30)$$

Describing a material in terms of its admittance emphasizes its ability to transport current. Alternatively, we could emphasize its ability to restrict the flow of current by considering its impedance  $Z^* = 1/Y^*$ , or for a pure conductance, its resistance,  $R = 1/G$ .

Factoring  $i\omega\epsilon_0$  in Equation 15.28 yields

$$I = \left( \epsilon_r - \frac{i\sigma}{\omega\epsilon_0} \right) i\omega\epsilon_0 A \cdot \frac{V}{d} = C \frac{dV}{dt} \quad (15.31)$$

We can define a complex-valued relative permittivity as

$$\epsilon^* = \epsilon_r - \frac{i\sigma}{\omega\epsilon_0} = \epsilon'_r - i\epsilon''_r \quad (15.32)$$

with

$$\epsilon'_r = \epsilon_r$$

$$\epsilon'' = \sigma/(\omega\epsilon_0)$$

The complex conductivity and complex permittivity are related by

$$\sigma^* = i\omega\epsilon^* = i\omega\epsilon_0\epsilon_r^* \quad (15.33)$$

In physical terms, we can consider the conductivity of a material as a measure of the ability of its charge to be transported throughout its volume due to the applied electric field. Similarly, its permittivity is a measure of the ability of its dipoles to rotate or its charge to be stored by an applied external field. Note that if the permittivity and conductivity of the material are constant, the displacement current will increase with frequency whereas the conduction current does not change. At low frequencies, the material will behave like a conductor, but capacitive effects will become more important at higher frequencies. For most materials, however, these material properties are not constant, but vary with the frequency of the applied signal.  $\sigma^*$  and  $\epsilon^*$  are frequency-dependent.

### 15.3.2 Biological Tissue in DC Electric Field

The electrical response of biological tissues when stimulated with DC electroporative pulses can be seen as quasi-stationary. Namely, for any material whose electric properties are in the range of those of biological tissues or organs and whose dimensions do not exceed 1 m and the frequency of the electric field is low, the electrical behavior in any given moment as a response to electric current can be numerically described with a set of equations describing stationary fields. Although the impedance of biological tissue has a capacitive component, the electric field can be considered as time independent, thus, the capacitive effects and the finite propagation of the electric current in the biological tissue are disregarded.

The electric field in a tissue and electric current passing through the tissue are coexisting and are related by Ohm's law (Equation 15.16). The corresponding integral values are electric current  $I$ , conductance  $G$  (which is the reverse of resistance  $R$ ), and voltage  $U$ . Ohm's law then takes the form of

$$U = R \cdot I \quad (15.34)$$

or

$$I = G \cdot U \quad (15.35)$$

Current passes through the tissue if a potential difference exists between two points in the tissue, and the current loop is closed. In practice, we generate the potential difference (voltage) on the electrodes with an electric pulse generator. When both electrodes (one needs at least two electrodes to close the loop) are placed on/in the tissue (which is a conductive material where charge carriers are ions as in electrolyte solutions), the current loop is closed and the current passes through the tissue.

As the electric current passes through a biological tissue, it is distributed through different parts of the tissue, depending on their electrical conductivity. In general, highly perfused tissues have higher conductivity; blood is highly conductive, as well as muscles, whereas bone and fatty tissue have low conductivity. The current will flow more easily and for the same voltage in higher proportion through more conductive tissues (e.g., muscles). On the contrary, the electric field in these tissues will be lower than in tissues with low conductivity for the same current.

Nevertheless, as the electric current takes the shortest and easiest path through the tissue, the current will be contained predominantly between the electrodes if they are close enough to each other. This property allows for relatively good control and containment of electric field distribution predominantly between the electrodes (Miklavčič et al. 1998).

Even though the pulses usually used in electroporation are DC, the capacitive properties of the biological material cannot always be disregarded. This holds true for the cases where the transient of cell membrane charging may also be interesting to study. Namely, cell membrane charging time is on the order of microseconds, and typical pulses used for electroporation of the cell membrane are 100  $\mu$ s long, with the amplitude of around 500 V/cm (Kotnik et al. 1997, 1998). It has been found that if pulses of much higher

amplitude (e.g., 50 kV/cm) and much shorter duration are used—in the order of tens of ns—the charging effect also becomes pronounced on the membranes of intracellular organelles (Schoenbach et al. 2001, Tekle et al. 2005, Kotnik and Miklavčič 2006). For a qualitative analysis of these processes, the time courses of organelle and cell plasma membrane charging become important. Thus, the capacitive component describing the electrical properties of the cell, its organelle(s), and their membranes can no longer be neglected.

### 15.3.3 Some Biological Tissue Properties Important in the Applied Use of Electroporation

#### 15.3.3.1 Tissue Anisotropy

When the properties of a material are the same in all directions, the material is said to be isotropic. However, some biological materials are distinctly anisotropic. Typical anisotropic tissues are, for example, skeletal muscle and tendon. Therefore, when referring to published electrical property data, the information about the orientation of the electrodes relative to the major axis of the tissue during impedance measurements is important (longitudinal, transversal, or a combination of both).

The conductivity of the material (in units: S/m) can, in the case of an anisotropic conductor, be represented by a tensor:

$$\sigma = \begin{bmatrix} \sigma_{xx} & \sigma_{xy} & \sigma_{xz} \\ \sigma_{yx} & \sigma_{yy} & \sigma_{yz} \\ \sigma_{zx} & \sigma_{zy} & \sigma_{zz} \end{bmatrix}$$

Whenever the material's conductivity can be described in the orthogonal Cartesian system and its spatial dependence can be aligned with the axes, the electric field and the current density can be described in the same way; the nondiagonal elements of the matrix equal zero, hence the matrix becomes diagonal:

$$\sigma = \begin{bmatrix} \sigma_{xx} & 0 & 0 \\ 0 & \sigma_{yy} & 0 \\ 0 & 0 & \sigma_{zz} \end{bmatrix}$$

If we take skeletal muscle for example, two different conductivity values can be measured in two different directions: one for the direction along the length of the muscle fibers and one that is perpendicular to it. If the muscle tissue is aligned with one of the axes of the coordinate system, two diagonal elements in the above matrix have the same value.

Tissue anisotropy is often related to the structure and physiological properties of the tissue. Skeletal muscles are composed of fibers that are very large, highly elongated individual cells and are aligned in the direction of muscle contraction. Electrical conduction along the length of the fiber is thus significantly easier than conduction between the fibers (the difference is about sevenfold) (Reilly 1998). The longitudinal conductivity is significantly higher than the transverse conductivity, especially in the low frequency range. Tissue anisotropy is also frequency-dependent (Hart et al. 1999). If the frequency of the current is high enough, the anisotropic properties disappear (specifically for skeletal muscle that happens in the MHz frequency range). At higher frequencies, charge movement takes place over shorter distances so large-scale structures become less important and capacitive coupling across membranes becomes more important.

#### 15.3.3.2 Nonlinear Behavior

With respect to the intrinsic characteristics of a system or equations describing it, an important consideration is whether the system is linear. Mathematically speaking, a nonlinear system does not satisfy the superposition principle stating that the response of a system caused by two or more input stimuli is the sum of the responses, which would have been caused by each stimulus individually. In terms of

equations, a nonlinear system is any system where the variable(s) to be solved for cannot be written as a linear sum of independent components. Unfortunately, most physical systems are inherently nonlinear in their nature and, unfortunately, biological tissues are not an exception. Often, the physical property of a material is changed during a process (material's temperature coefficients, conductivity changes during tissue electroporation). For some applications, a linear approximation of a nonlinear function can be found at (or around) a given point, for specific input values. However, if the model has to cover the whole (or larger) range of input values, the nonlinearities have to be considered in the model.

If we speak strictly about tissue properties exposed to electric current, at least two important nonlinearities need to be considered.

One is the increase in tissue conductivity ( $\sigma$ ) due to an increased electric field ( $E$ ) causing cell membrane electroporation (Pliquett and Weaver 1996, Pavšelj et al. 2005, Šel et al. 2005). This change of material properties has two more nonlinear characteristics. First, it is considered to be a threshold phenomenon, meaning that the electric field has to reach a certain value, termed reversible electropermeabilization threshold  $E_{rev}$ , in order to cause conductivity changes. Second, for the duration of the pulse, this conductivity change is an irreversible phase transition process. More specifically, once the conductivity is increased in a given tissue volume, it cannot be changed back to its lower value during pulse delivery, even if the electric field strength drops below the threshold due to changed conductivities. Here, we would like to point out that one has to be careful to distinguish between the reversibility of cell electroporation (provided the electric field was below the irreversible threshold) after the cessation of electric pulses; and the irreversible nature of the conductivity changes during pulse delivery—the change is only possible in one direction, tissue conductivity can only increase (Pavlin et al. 2005).

The second nonlinearity comes from the electrical–thermal coupling (Pliquett 2003). Once a part of a tissue is permeabilized, it becomes more conductive and the current density increases several times, causing resistive heating. In turn, tissue conductivity increases even more, as the temperature coefficient of electrical conductivity of most biological materials is positive—in the range of 1%–3%  $^{\circ}\text{C}^{-1}$  (Duck 1990).

### 15.3.3.3 Electric Field Threshold of Biological Tissues

The cell membrane is permeabilized when the threshold transmembrane potential is reached, thus, when the external electric field is above the threshold value. This increased cell membrane permeability is reversible, provided the electric field is not too high. However, if cells are exposed to an electric field above the irreversible threshold, they suffer permanent damage. For electroporation-based applications such as gene delivery (Golzio et al. 2004, André et al. 2008) or transdermal drug delivery (Prausnitz 1999, Denet and Préat 2003, Denet et al. 2004), this is not a desirable effect as the cells have to be viable after the treatment. On the other hand, for applications based on irreversible electroporation, the target cells can be irreversibly destroyed within a narrow range while leaving neighboring cells unaffected. This technique represents a promising new treatment for cancer, heart disease, and other conditions that require tissue ablation (Davalos et al. 2005, Lavee et al. 2007, Onik et al. 2007, Rubinsky et al. 2007).

In any case, it is important to determine the needed amplitude of electric pulses at a given electrode-tissue setup to achieve an electric field distribution in the tissue that is adequate for a given application. Electric field reversible and irreversible thresholds are both inherent characteristics of the tissue (also different for different tissues), no matter what kind of electrodes we use or if inhomogeneous or composed tissues are involved. Of course, the electropermeabilization process as well as cell viability depend on electrical parameters, i.e., pulse amplitude, pulse duration, and the number of pulses (see [Figure 15.1](#)) (Maček-Lebar et al. 2002, Puc et al. 2003).

However, accomplishing an adequate electric field distribution in the tissue is much more complex than merely calculating the voltage we need at a given electrode separation ( $U/d$ ). Mathematically, this ratio gives an electric field only when delivering pulses to a homogeneous tissue through parallel plate electrodes whose surface is large (infinite) compared with the electrode separation (see [Figure 15.2a](#)). It can still be used as an approximation of the electric field in the area between the parallel plate electrodes

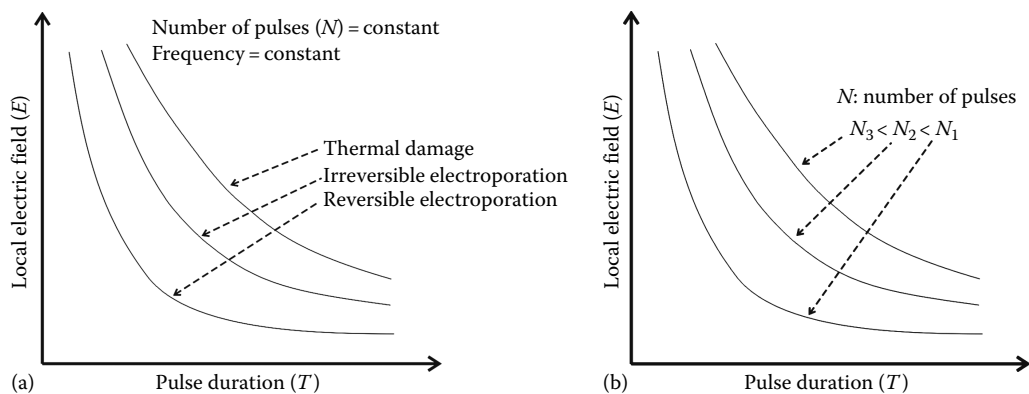


**FIGURE 15.1** Electroporation process is (for a given tissue-electrode geometry) controlled by pulse parameters. (a) At constant number of pulses ( $N$ ) and their frequency, lengthening pulse duration requires lower local electric field (pulse amplitude) for the same effect. If both are increased, the effects on the tissue become irreversible, or, at even higher values, tissue thermal damage can be observed, due to excessive resistive heating. (b) Similarly, for any of the curves, if number of applied pulses is larger, the same effect can be achieved with a lower pulse amplitude and/or duration.

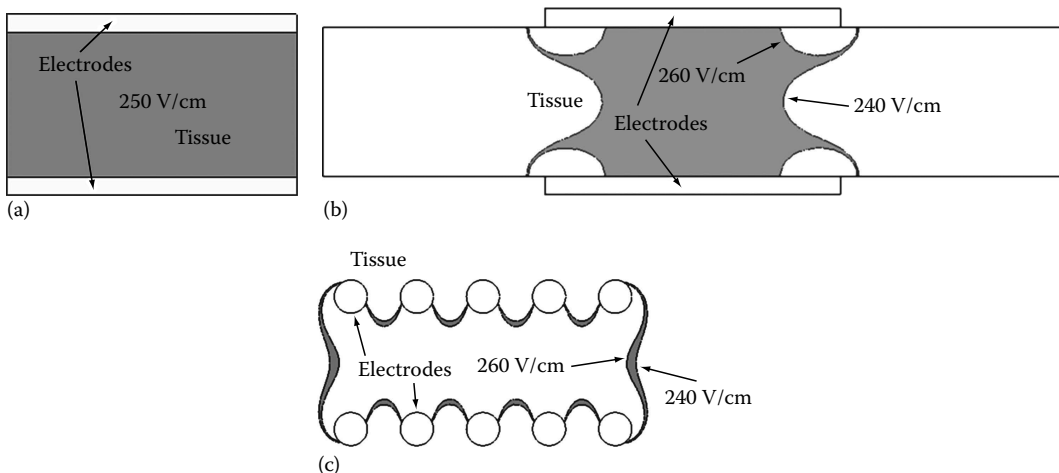


**FIGURE 15.2** Curves of the same electric field in a homogeneous tissue in a section plane perpendicular to electrodes. (a) The electric field equals the ratio  $U/d$  (voltage/distance between electrodes) only in the theoretical case where electric pulses are delivered through plate electrodes of infinite surface. Here, only a portion of this infinite structure is modeled with boundary conditions set to represent an infinite volume. The distance between the electrodes ( $d$ ) is 4 mm, the applied voltage ( $U$ ) is 100 V, and thus the electric field equals  $U/d = 250$  V/cm throughout the tissue between the electrodes. (b) A real situation where electrodes are of finite dimension. The electric field in the gray area between the two black isocontours is between 240 and 260 V/cm, so the voltage to distance ratio in this area is a good approximation, except near the edges of the electrodes. The  $U/d$  approximation is valid in a greater portion of the tissue between the electrodes if the electrode surface is increased or the distance between them is smaller. (c) Two rows of needle electrodes are used instead of plate electrodes. The length of the electrode array and the distance between the rows is the same as in (b). The gray area between the two black isocontours denoting electric field between 240 and 260 V/cm is very small and limited to a few narrow stripes. Throughout most of the area inside the electrode array the electric field is higher (around 300 V/cm or higher) and thus cannot be satisfactorily approximated by voltage to distance ratio.

of finite dimensions, away from their edges (Figure 15.2b). The  $U/d$  ratio is also often used to estimate the electric field between two parallel rows of needle electrodes. Some are referring to the  $U/d$  ratio as a “nominal” field; however, the approximation is extremely rough (Figure 15.2c). In the case of any other electrode geometry using plate, needle, microneedle, or surface electrodes or if more than one tissue is involved, a numerical analysis has to be performed beforehand, as a part of treatment planning, in order to choose the right electrode configuration and the pulse amplitude.

## 15.4 Modeling

---

Having acquired some basic knowledge about the electromagnetic field theory and specificities of biological tissues, we can set about constructing mathematical models representing different aspects of electroporation.

The starting point of the modeling process is deciding on the mathematical approach to adequately describe the modeled system by first acquiring enough observable and measurable information about it. Typically, more than one modeling approach is possible and choosing the most suitable one depends on the modeler’s or end user’s objective needs and personal preferences, as well as the physical and geometrical characteristics of the modeled system. In some cases, using more than one modeling approach can be beneficial in terms of model verification and validation. More than one phenomenon can determine a system, which is especially the case with biological systems. Generalizations and simplifications are possible and, in most cases, cannot be avoided. The model can refer only to some aspects of the real system, while disregarding the ones that either have a very limited influence on its accuracy or are out of the scope of this particular model. Prior to building a model, we need to define its scope, apply necessary simplifications while being aware of the circumstances or the range of input variables for which the model is valid.

Deciding on the right level of complexity for our model is not always an easy task as it involves a trade-off between simplicity and accuracy. As a general guideline, if we are choosing from different models giving comparable results, the simplest one is the most desirable. Namely, we need to be aware that adding complexity can make the model difficult to understand and experiment with and can pose computational problems.

Analytical methods are rather complicated and are only feasible for use on problems where the geometry, material properties, and boundary conditions can easily be described in a defined coordinate system (Cartesian, cylindrical, or spherical). Simple analytical models can have certain advantages over numerical models. First, the input data needed is typically less extensive than that of numerical models. Also, analytical solutions have no numerical and discretization errors. The obvious limitation of analytical models is that only the simple and uniform geometries, boundaries, and initial conditions can easily be modeled. In the last decades, analytical models have mostly been replaced by numerical models based on boundary element, finite difference, finite volume, or finite element methods, due to the miniaturization and accessibility of both computer hardware and software. Of these methods, the latter is preferred in the modeling of electroporation, due to its relatively easy implementation and its ability to handle more intricate geometries. The principle behind this method is the discretization of the geometry into smaller elements where the quantity to be determined is approximated with a function or is assumed to be constant throughout the element. Discrete elements can be of different shapes and sizes, which allows for the modeling of intricate geometries. In such models, the excitations can be changed easily, being that it only involves changing the boundary conditions on the same model. The model geometry, however, takes time and precision to be built and generalizations and simplifications need to be used when possible.

### 15.4.1 Building a Geometry

When designing a numerical model, we must decide for the appropriate details to be included. Geometrically more detailed models will inevitably consume more of both the modeler’s and the

computer's time, but do not necessarily produce better quality results, as the inclusion of geometrical details depends on the purpose of the model.

#### 15.4.1.1 Geometrical Symmetries

Taking advantage of the geometrical symmetries of the system we are modeling allows us to analyze a structure or a system by modeling only a portion of it by applying appropriate boundary conditions. This approach can be used when the same symmetry can be observed in both the geometry as well as the sources (in our case of electric current). It reduces the size of the model and consequently the analysis run time as well as the demands on computer resources. Alternatively, modeling only a portion of the whole geometry allows us to include more details in the model, when needed, thereby obtaining better results that would not have been possible with the full geometry (Pavšelj et al. 2007). For example, when representing a tumor with a simplified elliptical shape, supposing also the symmetry of the electric stimulation), only a quarter of the tumor can be modeled (see Figure 15.3a). A similar approach can be used when modeling a geometrical structure with a repetitive infinite or quasi-infinite pattern (Figure 15.3b). In this case, only a small portion of the whole array, a unit cell, needs to be modeled by applying the appropriate periodic boundary conditions (Susil et al. 1998, Pavlin et al. 2002).

Similarly, sometimes we are able to represent a 3D structure by a single 2D plane. For example, in Cartesian coordinates, a structure stretched along a straight line (Z-direction) can be represented with a structure in the X-Y plane, while the model is assumed to be uniform in the perpendicular Z-direction (see Figure 15.4a). Similarly, if the structure is axisymmetrical, the plane of symmetry is the cross section anywhere around the axis of symmetry. In this case, we are using a single 2D slice ( $r-z$  cylindrical coordinates) to represent the whole  $360^\circ$  of the structure (see Figure 15.4b).

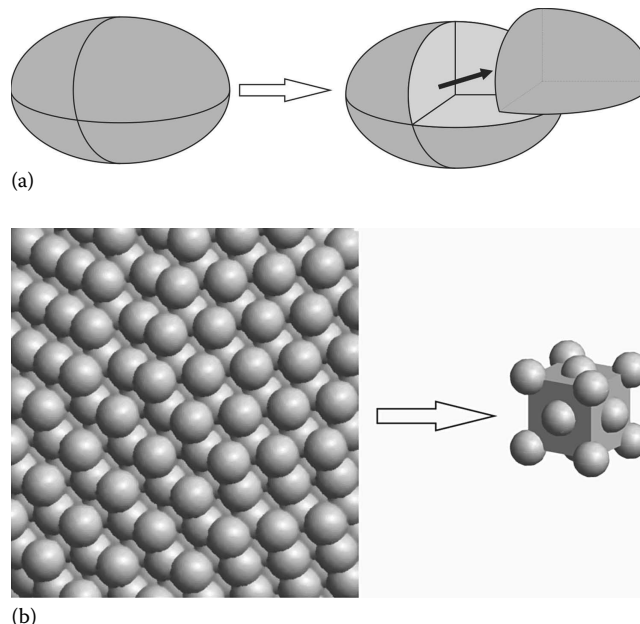


**FIGURE 15.3** Representation of a large structure with only a portion of its geometry. (a) When modeling an elliptically shaped tumor during electrochemotherapy, supposing the electric stimulation exerts the same symmetry, only a quarter of the tumor need be modeled. (b) A finite representation of an infinite 3D lattice, such as cells in a cluster.

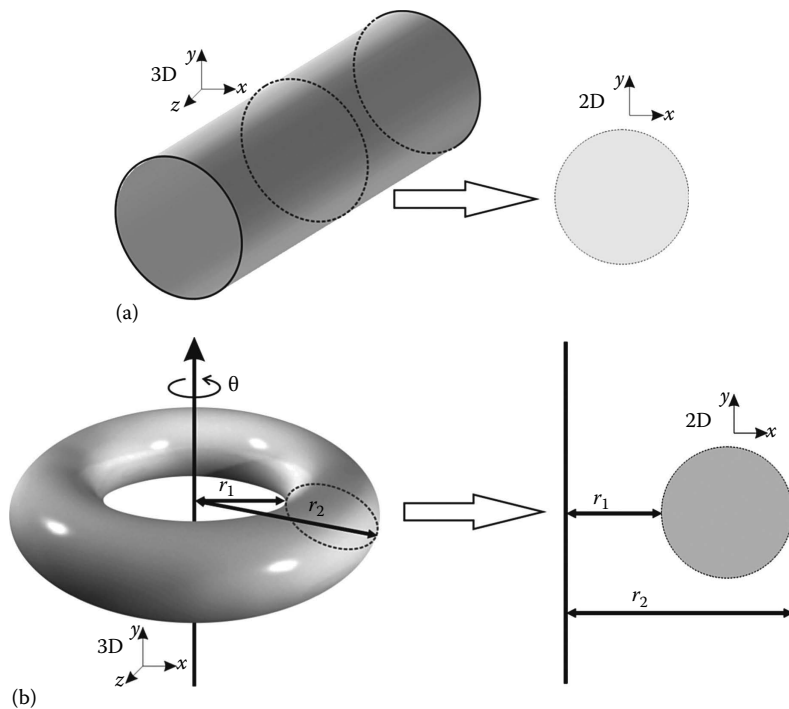


**FIGURE 15.4** Representation of a 3D structure by a single 2D plane. (a) 2D representation of a 3D geometry. In this case, the cylinder was represented by its cross section. (b) 2D representation of a 3D axisymmetrical structure.

#### 15.4.1.2 The Size of the Modeled Volume/Area

In some cases, the modeled system has no borders electrically insulating it from its surroundings; the electrical quantities are simply diminishing with increasing distance from the source. One such example is needle electrodes inserted in a tissue (Figure 15.5). In such cases, the outer boundaries of the model need to be far enough from the source(s), in order not to restrain the natural flow of the electric current (see Figure 15.5a). Namely, when modeling such a system, the borders of the model are artificially electrically insulated from the surroundings. This effectively means that the boundary condition is set in such a way that no electric current flows in or out of the enclosing box—only tangential components of the electric current exist on the outer tissue borders while the normal component equals zero. If these borders are too close to the source(s) of the electric current, such as in Figure 15.5b, the electric field and current distribution is deformed and does not reflect the true situation. The safest way to choose the right distance of the model borders from the source(s) is by changing the dimensions of the enclosing box and observing its effect on the results. The enclosing box is large enough when, if further increased, the effect on the calculated scalar and vector fields is negligible.

#### 15.4.1.3 Modeling of Biological Entities

Numerous examples could be given to illustrate either the importance or futility of including physiological details in the geometry of the model. Already at the cell level, *in vitro* observations on cell suspensions can be represented numerically on different levels. For example, when studying the magnitude and the distribution of the electric field in a cell suspension, a material with homogeneous properties is an adequate model (Pavlin and Miklavčič 2003). However, if the aim of our research is to study the phenomena on the cell level or if we are looking into interactions between cells, the influence of their size, shape, density, and orientation, individual cells rather than bulk material have to be modeled (Susil et al. 1998, Pavlin et al. 2002, Valič et al. 2003, Pucihař et al. 2006, Pavlin and Miklavčič 2008, Towhidi et al.

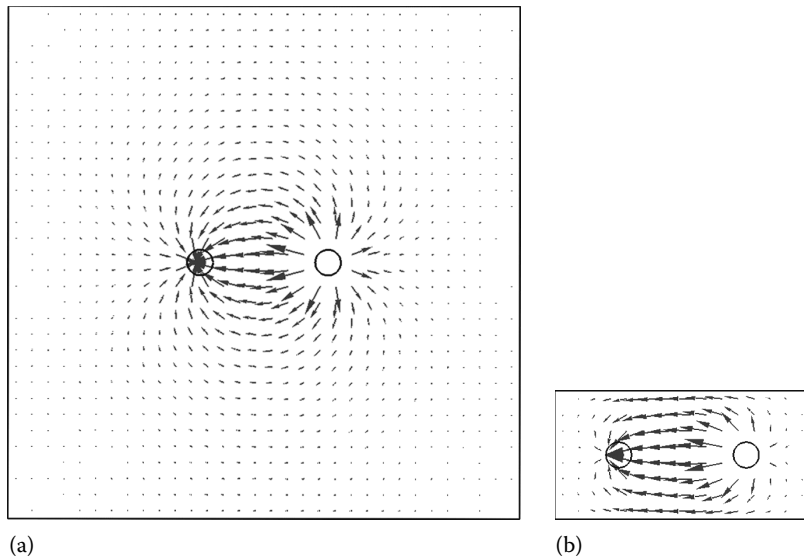


**FIGURE 15.5** The electric current density— $J$  (gray arrows) in a homogeneous material, electric pulse is delivered through needle electrodes (the two black circles). The electric current density is shown in a section plane cut through the material, perpendicular to electrodes. (a) The insulated borders of the model are far enough from the electrodes, which allows for the natural flow of the electric current, the electric field and the electric current near model borders are very close to zero. (b) The borders of the model are too close to the electrodes, the electric field close to the border is not zero, electric current is artificially constrained.

2008). Even further, if we are using nanopulses, cell organelles must be added to the geometry (Kotnik and Miklavčič 2006). Still, by using smart approaches, such as replacing a thin, non-zero conductivity cell membrane by a boundary condition between the cytoplasm and the exterior, getting rid of complexities while maintaining accuracy of the model is possible (Pucihar et al. 2006).

Similar observations hold true on the tissue level. Different levels of complexity and inhomogeneity can be observed in different tissues; however, including their particularities depends strongly on the purpose of the model. Skin, for example, is a very intricate tissue due to its highly inhomogeneous structure, leading to inhomogeneous electric properties. It consists of different layers in terms of dimensions (thickness) and electrical properties: the outer thin layer of dead flat skin cells, the stratum corneum, the viable epidermis, dermis, and the subcutaneous tissue (Yamamoto and Yamamoto 1976a,b, Chizmadzhev et al. 1998). If the aim of the model is to study the electroporation of skin as a target tissue, this layered structure needs to be included in the geometrical representation (Pavšelj et al. 2007). Moreover, even this bulk layered structure might sometimes prove inadequate. Smaller structures, such as hair follicles, sweat glands, and blood vessels, or local transport regions as a result of skin electroporation (Pavšelj et al. 2008a) may have to be added in order to study the processes on the microscale, where they occur, and only then compare them to bulk observations. On the one hand, such details, unavoidably adding to the overall complexity of the model, can be omitted in cases where skin electroporation is not studied directly, such as any application where electric pulses are delivered with external electrodes to tissues beneath the skin (Pavšelj et al. 2005). On the other hand, other structures, such as major blood vessels may be important and need to be included in the model when studying the mechanisms of the electrochemotherapy of tumors (Serša et al. 2008).

### 15.4.2 Setting the Physics of the Model

After the geometry of the model has been constructed, the next step in the modeling process is setting the physics of the model, such as underlying equations, material properties, boundary, and initial conditions.

### 15.4.2.1 Frequency-Dependent Component

First, the material's response will be different when exposed to either direct (DC) or alternating current (AC). If our material is purely resistive, the system exerts no frequency dependency; the current is proportional to the voltage irrespective of the frequency. However, in general, materials have their capacitive or inductive component so the voltage to current ratio does depend on frequency and is termed impedance ( $Z$ ). Impedance is a complex quantity consisting of a resistance  $R$  (the real part) and a reactance  $X$  (the imaginary, frequency-dependent part):

$$\vec{Z} = R + jX \quad (15.36)$$

The resistance can only be positive, while the reactance can be either positive (inductive character, current lagging behind voltage— $X_L$ ) or negative (capacitive character, voltage lagging behind current— $X_C$ ).

$$X_L = j\omega L \quad (15.37)$$

$$X_C = -j \frac{1}{\omega C} \quad (15.38)$$

Voltage and current can be considered as vectors in the complex plane (phasors) that are out of phase, so the voltage to current ratio—the impedance—can also be given by its magnitude and phase angle:

$$\vec{Z} = |Z| \cdot e^{j\Theta} \quad (15.39)$$

$$|Z| = \sqrt{R^2 + X^2} \quad (15.40)$$

$$\Theta = \arctg \frac{X}{R} \quad (15.41)$$

Resistance is only a special case of impedance, when the material we are considering exerts no or negligible capacitive or inductive character ( $jX = 0$ ). Further, if a system is exposed to DC, the frequency-dependent part—the reactance  $X$ —plays no role when the system is in steady-state, after all the transients have faded out. It does, however, dictate the course of the transient of the system, which poses the next question in the modeling process: Are we interested only in the steady-state of our system or are we studying transient phenomena—changes over time from  $t = 0$  until the system has reached its steady-state?

### 15.4.2.2 Transient vs. Steady-State

Transient behavior occurs when the magnitude and direction of electrical quantities change with time. On the contrary, if they are constant with time throughout the entire volume, the system is already in its steady-state. To avoid any ambiguity, the steady-state does not mean the absence of movement or flow in the system! If we take electric currents in a material as an example, it simply means that the “amount” of electric current in the system does not change within an observed time; the magnitude of the current exiting the system equals the current magnitude flowing into the system at any time when in steady-state. In other words, time becomes an irrelevant variable for the analysis, since the recently observed behavior of the system will continue into the future.

In many systems, steady-state is not achieved until sufficient time has elapsed after the system is started or stimulated (externally or internally). The situation after the occurrence of the described changes of the system and before all internal quantities (states) of the system reach the steady-state is defined as the transient state. As an example, in an electrical system of purely resistive character, no transients occur at  $t = 0$ , when the electrical stimulation is turned on. However, if the imaginary part (the reactance) is present in the impedance of the electrical system, its behavior exerts inertia, meaning that the change of electrical quantities in the system is not instantaneous. The capacitive or the inductive

component opposes the sudden change at  $t = 0$  (applied voltage or current) and enforces the transient state onto the system that will, however, eventually fade out.

#### 15.4.2.3 Multiphysics

The effects of various physical phenomena can be investigated by separately analyzing each individual phenomenon without any consideration of the interaction between them. However, often we are dealing with two or more interacting, simultaneous phenomena, such as the coupling between the electric and the magnetic fields. An important coupling of physical phenomena in applications using electric pulses on biological tissues is heat transfer in tissue due to resistive heating (Tungjitusolmun et al. 2000). This coupling may give rise to tissue conductivity changes (due to temperature increase), which in turn change the magnitude of the electric current. When constructing a model, the influence of such interactions have to be estimated and, if needed to obtain accurate results, mutual dependencies have to be included. To do so, we need data on how the material properties significant for one field (such as the electric field) vary with the magnitude of another field (such as temperature) and vice versa.

#### 15.4.3 Interpretation of Results

When modeling the electroporation of biological tissues, much consideration has to be given to the interpretation of the results in relation to possible simplifications in the model or inherent characteristics of different biological tissues. Namely, some simplifications might not have much effect in isotropic, homogeneous tissues, such as the liver, but may yield useless results in inhomogeneous, composed biological structures, such as layered skin or subcutaneous tumors, where electric field distribution is much more complex (Pavšelj et al. 2005, Ivorra et al. 2008, Pavšelj and Miklavčič 2008b). To illustrate, when modeling electroporation in a homogeneous tissue, such as the liver, the results are still useful and comparable to experimental data even if the conductivity increase due to tissue electropermeabilization is neglected. In fact, early models did not take this nonlinear tissue behavior into account (Miklavčič et al. 2000). However, when more complicated electrode-tissue setups were being studied with numerical models, experimentally observed phenomena could not be satisfactorily modeled in this way. Namely, upon applying electric pulses on a composed or layered tissue with an inhomogeneous distribution of electrical conductivities, the voltage is divided among them proportionally to their electrical resistances (Pavšelj and Miklavčič 2008b). This leads to a more complex electric field distribution, meaning that some parts of the tissue, due to their low electrical conductivity (disproportionally lower than the rest of the tissue), are exposed to a much stronger electric field. The electric field is the highest in the layer with the highest resistivity (lowest conductivity). In the case of the subcutaneous tumor, this is the skin, which has the lowest electrical conductivity, and in the case of the skin fold, the highest electric field is in the nonconductive outermost skin layer, the stratum corneum. But more importantly, the electric field in the target tissues (tumor and viable skin layers) stays too low for successful electroporation. This fact raised the question of how the experimentally confirmed successful permeabilization of the target tissues theoretically is possible when external plate electrodes are used, which led to the inclusion of tissue conductivity changes due to electroporation in the numerical models.

#### 15.4.4 Model Verification and Validation

The last, but nevertheless very important part of the modeling process is the verification and the validation of the constructed model, involving different aspects of evaluation. Mostly, these aspects should be taken into consideration from the very beginning of the process and can roughly be divided into three categories:

1. *Verification:* The main question here is whether we reached the aim of the model. Already in the planning phase of the modeling process, we have to set the scope of our model, the range of input data it should be valid for, as well as geometrical details to be included. However, as we build the model, some simplifications and trade-offs may have to be made. Comparing the actual result

with the requirements set during the planning phase will demonstrate whether our resulting model is still within the planned scope of the model or not.

2. *Descriptive realism:* Have we identified and explained the underlying physics? In cases where almost nothing is known about the phenomena describing the modeled system, we are dealing with the so-called black box problem that can only be treated in terms of its input and output characteristics. Our only option may be finding a curve that has the best fit to a series of data points, while respecting possible constraints without actual physical reference to the described process(es). However, different techniques of system identification (Ljung 1999) can be applied in order to identify the physics defining our “black box,” which can then be modeled. Namely, the purpose of modeling is to gain insight and explain underlying phenomena, as well as using them for predicting the output at certain input data sets. We should therefore direct our efforts to turn the black box into a set of equations, if possible. Once again, as some trade-offs will most likely be necessary, we should assess if the modeled physical phenomena successfully explain the most important experimental observations.
3. *Validation:* Does our model agree with the empirical data? One way to justify the physics used in the model (sometimes the only way) is by comparing the output data obtained from the model to experimental data. Usually, or ideally, the experimental data can be divided into two groups: the training data and the validation data. The former is used to identify the process and to construct a model with its relevant parameters and constraints, while the latter is used to assess if the model is valid for any range of input parameters within the defined constraints.

## 15.5 Treatment Planning

---

When electroporation is used in biomedical experiments and medical treatments, the (steady-state) electric field distribution inside the target tissues is one of the most important predictors of success (Miklavčič et al. 1998). Models have helped us to understand that the electric field in tissue changes its magnitude during pulses, as the conductivity increases due to electroporation (Pavšelj et al. 2005, Šel et al. 2005). Also, modeling has shown the importance of ensuring good surface contact between the electrodes and tissue, when plate electrodes are used to deliver electric pulses (Čorović et al. 2008a), and the importance of the depth of insertion, when needle electrodes are used (Čorović et al. 2008b). It has also been shown that for a known number and duration of applied electric pulses, the electric field has to be higher than a threshold value ( $E > E_{th}$ ) for electroporation to occur (Šemrov and Miklavčič 1998). As such, the electric field distribution can serve as a predictor of treatment outcome. As has been mentioned in the previous sections, the local electric field distribution inside biological tissue is very hard to predict without numerical models. If a specific distribution is needed, as is the case in electroporation-based medical treatments, several attempts are needed before the right electrode positions relative to the target tissue and voltages between the electrodes are found. The more complex the case, the more time is needed to determine the treatment parameters by trial and error (forward planning), therefore, numerical optimization techniques (inverse planning) have to be used: a desired electric field distribution can be set and appropriate treatment parameters (electrode positions, voltages) can be determined by numerical optimization (Županić et al. 2008).

In practice, these more complex cases include target tissues that are located deep in the body or close to the vital organs. In such cases, it is important to control the magnitude and distribution of the electric field so that a minimum volume of vital tissue is compromised by the treatment. Numerical modeling may also be necessary for treatment planning in tissues with highly anisotropic properties and highly nonhomogeneous tissues (Pavšelj and Miklavčič 2008b). In such cases, the treatment planning procedure has to be applied individually for each patient and the electric field distribution has to be sculpted carefully to guarantee that the entire target tissue is exposed to a high enough electric field, while vital tissues are as unaffected as possible.

Treatment planning does not consist solely of optimization and modeling, but is instead an integral part of the whole treatment process. Normally, medical imaging (CT, MRI) is first used to obtain

information about the anatomical details of the treated volumes. The images are converted into mathematical representations and used in the numerical model to calculate the electric field distribution. The numerical model is used in the optimization algorithm to calculate the best treatment parameters (electrode positions and voltages). Additional measures can be taken to ensure that the treatment plan is successfully executed, e.g., the insertion of electrodes can be controlled by ultrasound imaging and the extent of electroporation can be monitored by current and voltage measurements (Cukjati et al. 2007) or electrical impedance imaging (Davalos and Rubinsky 2004, Ivorra and Rubinsky 2007). Therefore, it can be argued that the quality of numerical treatment planning for electroporation-based treatment depends on the quality of medical imaging, target and normal tissue identification, detailed knowledge of the biological effects of the electric field (changes in tissue properties, threshold values), and the quality of the underlying model. At present, not all of the requisites are met. For one, electroporation thresholds are tissue specific and are not yet readily available. Furthermore, several electric pulse parameters that affect the threshold values: pulse duration, number of pulses, and to some extent also pulse repetition frequency (Pucihar et al. 2002, Edd and Davalos 2007) have not yet been included in numerical models. Therefore, prior to any treatment planning, data on thresholds for all relevant tissues should be available for a range of electroporation parameters.

We present an example of treatment planning of the electrochemotherapy of a tumor nodule located near a vital organ using numerical modeling and a genetic optimization algorithm. The goal is to determine the best possible configuration and electric potentials of six electrodes surrounding a subcutaneous tumor—the target tissue. The treatment parameters must irreversibly electroporate ( $E > E_{\text{rev}}$ ) the entire tumor volume while sparing the hypothetical spherical vital organ ( $E < E_{\text{irr}}$ ) situated next to the tumor (Figure 15.6).

The steady-state numerical model of electroporation is used, taking into account the changes in tissue conductivities because of electroporation; i.e., electric field distribution in the tissue caused by an electric pulse is determined by solving the Laplace equation for static electric currents (2.19) with  $\sigma(E)$ . All tissues are considered isotropic and homogeneous. The assigned conductivity values and electroporation thresholds are given in Table 15.1. These values are mostly taken from existing literature (Gabriel et al. 1996a,b, Davalos et al. 2005, Pavšelj et al., 2005, Cukjati et al. 2007) or, in cases where data cannot be found in existing literature, are educated guesses, meant only for demonstration purposes.

A genetic algorithm is used for the optimization procedure. A population of possible solutions (treatment plans consisting of the positions and direction of each electrode  $[x, y, z, \phi, \theta]$  and all used voltages) is first randomly chosen. The solutions then evolve in iterations by mathematical operation cross-over and mutation according to their fitness function

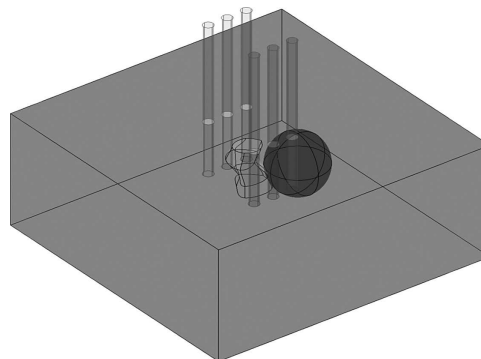


**FIGURE 15.6** Model geometry: healthy tissue, tumor (between the electrodes)—geometry taken from Šel et al. (2007), vital organ (sphere). Needle electrodes are inserted into the tissue and appropriate electric potentials are assigned to each electrode so that the entire tumor volume is reversibly electroporated and the least possible volume of the vital organ is irreversibly electroporated.

**TABLE 15.1** Tissue Properties Used in the Numerical Model

Tissue	$\sigma_1$ (S/m)	$\sigma_2$ (S/m)	$E_{rev}$ (V/m)	$E_{irr}$ (V/m)
Tumor	0.2	0.7	400	900
Vital organ	0.15	0.5	250	600
Healthy tissue	0.15	0.5	250	600

$$F = 10 \cdot V_{Trev} - 2 \cdot V_{VOir}, \quad (15.42)$$

where

$F$  is the fitness

$V_{Trev}$  is the fraction of tumor volume subjected to local electric fields above reversible thresholds ( $E > E_{rev}$ )

$V_{VOir}$  is the fraction of volume of the organ at risk subjected to  $E > E_{irrev}$

The weights in the fitness function (importance factors) are set arbitrarily, but with respect to the importance of the individual parameters for efficient electroporation. Namely, the most important endpoint of the treatment is the reversible electroporation of the entire tumor (weight 10 in Equation 15.42), while sparing the vital organ is not as important (weight 2). In the clinical environment, these importance factors would have to be set by an experienced physician. In our case, the algorithm optimizes 36 different parameters (positions  $[x, y, z, \phi, \theta]$  and electric potentials of all six electrodes). It is presumed that it is possible to achieve a good enough electric field distribution using these parameters.

The final treatment plan is presented in Figure 15.7. The resulting electric field distribution is not at all homogeneous; the field around the electrodes and in some parts of the tumor is much higher than in other parts of the tissue. Nevertheless, the tumor is completely reversibly electroporated, while 0.3% of the vital organ is irreversibly electroporated. From that we can conclude that the treatment planning goals have been met.

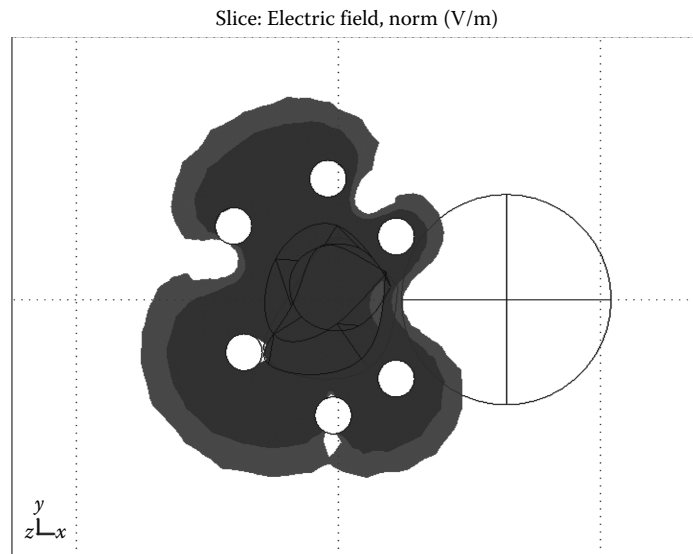


**FIGURE 15.7** Electric field distribution for the treatment plan 2 is shown in the  $XY$  plane through the center of the tumor. Light gray areas are reversibly electroporated ( $E > E_{rev}$ ), while dark gray areas are irreversibly electroporated ( $E > E_{irr}$ ).

## 15.6 Summary

This chapter explains in detail the process of electric field distribution modeling in biological tissues. The equations used in modeling are derived from Maxwell's equation of the electromagnetic field, while taking into account the dynamics of the induced transmembrane potential compared with the duration of electric pulses and the behavior of biological tissue in the presence of external electric fields. Biological tissues, which can be heterogeneous, anisotropic, and nonlinear, are included in the equations in the form of electric fields and direction-dependent tissue properties. The model geometry has to be chosen carefully, according to the modeling aims—the simplest possible geometry and form of equations that give good results should be used to make the calculation as fast as possible and also easier to interpret. Finally, the numerical modeling of electric field distribution is not only useful for explaining the experimental results and hypothesis testing, but also in the clinical setting, where it can be used together with optimization techniques in the inverse treatment planning of electroporation-based treatments.

## Acknowledgments

The authors would like to thank the Slovenian Research Agency and the European Commission for financial support.

## References

- André F, Gehl J, Serša G, Préat V, Hojman P, Eriksen J, Golzio M et al. 2008. Efficiency of high- and low-voltage pulse combinations for gene electrotransfer in muscle, liver, tumor, and skin. *Human Gene Ther* 19:1261–1271.
- Brandisky K, Daskalov I. 1999. Electrical field and current distributions in electrochemotherapy. *Bioelectrochem Bioenerg* 48:201–208.
- Chizmadzhev YA, Indenbom AV, Kuzmin PI, Galichenko SV, Weaver JC, Potts RO. 1998. Electrical properties of skin at moderate voltages: Contribution of appendageal macropores. *Biophys J* 74:843–856.
- Čorović S, Al Sakere B, Haddad V, Miklavčič D, Mir LM. 2008a. Importance of contact surface between electrodes and treated tissue in electrochemotherapy. *Technol Cancer Res Treat* 7:393–399.
- Čorović S, Županić A, Miklavčič D. 2008b. Numerical modeling and optimization of electric field distribution in subcutaneous tumor treated with electrochemotherapy using needle electrodes. *IEEE Trans Plasma Sci* 36:1665–1672.
- Cukjati D, Batiuskaite D, André F, Miklavčič D, Mir LM. 2007. Real time electroporation control for accurate and safe in vivo non-viral gene therapy. *Bioelectrochemistry* 70:501–507.
- Davalos RV, Rubinsky B. 2004. Electrical impedance tomography of cell viability in tissue with application to cryosurgery. *J Biomech Eng* 126(2):305–309.
- Davalos RV, Mir LM, Rubinsky B. 2005. Tissue ablation with irreversible electroporation. *Ann Biomed Eng* 33(2):223–231.
- Debruin KA, Krassowska W. 1999a. Modeling electroporation in a single cell. I. Effects of field strength and rest potential. *Biophys J* 77:1213–1224.
- Debruin KA, Krassowska W. 1999b. Modeling electroporation in a single cell. II. Effects of ionic concentrations. *Biophys. J.* 77:1225–1233.
- Denet A-R, Préat V. 2003. Transdermal delivery of timolol by electroporation through human skin. *J Control Release* 88:253–262.
- Denet A-R, Vanbever R, Préat V. 2004. Skin electroporation for transdermal and topical delivery. *Adv Drug Deliv Rev* 56(5):659–674.
- Dev SB, Dhar D, Krassowska W. 2003. Electric field of a six-needle array electrode used in drug and DNA delivery in vivo: Analytical versus numerical solution. *IEEE Trans Biomed Eng* 50(11):1296–1300.

- Duck FA. 1990. *Physical Properties of Tissue: A Comprehensive Reference Book*. Academic Press, London, U.K.
- Edd JF, Davalos RF. 2007. Mathematical modeling of irreversible electroporation for treatment planning. *Technol Cancer Res Treat* 6(4):275–286.
- Fear EC, Stuchly MA. 1998. Modeling assemblies of biological cells exposed to electric fields. *IEEE Trans Biomed Eng* 45(10):1259–1271.
- Foster KR, Schwan HP. 1989. Dielectric properties of tissues and biological materials: A critical review. *Crit Rev Biomed Eng* 17:25–104.
- Gabriel C, Gabriel S, Corthout E. 1996a. The dielectric properties of biological tissues: I. Literature survey. *Phys Med Biol* 41:2231–2249.
- Gabriel S, Lau RW, Gabriel C. 1996b. The dielectric properties of biological tissues: II. Measurements in the frequency range 10 Hz to 20 GHz. *Phys Med Biol* 41:2251–2269.
- Golzio M, Rols MP, Teissié J. 2004. In vitro and in vivo electric field-mediated permeabilization, gene transfer, and expression. *Methods* 33(2):126–135.
- Grimnes S, Martinsen OG. 2000. *Bioimpedance & Bioelectricity Basics*. Academic Press, London, U.K.
- Hart FX, Berner NJ, McMillen RL. 1999. Modelling the anisotropic electrical properties of skeletal muscle. *Phys Med Biol* 44:413–421.
- Ivorra A, Rubinsky B. 2007. In vivo electrical impedance measurements during and after electroporation of rat liver. *Bioelectrochemistry* 70(2):287–295.
- Ivorra A, Al-Sakere B, Rubinsky B, Mir LM. 2008. Use of conductive gels for electric field homogenization increases the antitumor efficacy of electroporation therapies. *Phys Med Biol* 53:6605–6618.
- Kotnik T, Miklavčič D. 2006. Theoretical evaluation of voltage induction on internal membranes of biological cells exposed to electric fields. *Biophys J* 90:480–491.
- Kotnik T, Bobanović F, Miklavčič D. 1997. Sensitivity of transmembrane voltage induced by applied electric fields—A theoretical analysis. *Bioelectrochem Bioenerg* 43:285–291.
- Kotnik T, Miklavčič D, Slivnik T. 1998. Time course of transmembrane voltage induced by time-varying electric fields—A method for theoretical analysis and its application. *Bioelectrochem Bioenerg* 45:3–16.
- Lavee J, Onik G, Mikus P, Rubinsky B. 2007. A novel nonthermal energy source for surgical epicardial atrial ablation: Irreversible electroporation. *Heart Surg Forum* 10(2):96–101.
- Ljung L. 1999. *System Identification—Theory for the User*, 2nd edn., PTR Prentice Hall, Upper Saddle River, NJ.
- Maček-Lebar A, Serša G, Kranjc S, Grošelj A, Miklavčič D. 2002. Optimisation of pulse parameters in vitro for in vivo electrochemotherapy. *Anticancer Res* 22:1731–1736.
- Miklavčič D, Beravs K, Šemrov D, Čemažar M, Demšar F, Serša G. 1998. The importance of electric field distribution for effective in vivo electroporation of tissues. *Biophys J* 74:2152–2158.
- Miklavčič D, Šemrov D, Mekid H, Mir LM. 2000. A validated model of in vivo electric field distribution in tissues for electrochemotherapy and for DNA electrotransfer for gene therapy. *Biochim Biophys Acta* 1523:73–83.
- Miklavčič D, Čoročić S, Pucihař G, Pavšelj N. 2006a. Importance of tumour coverage by sufficiently high local electric field for effective electrochemotherapy. *Eur J Cancer Suppl* 4:45–51.
- Miklavčič D, Pavšelj N, Hart FX. 2006b. *Electric Properties of Tissues*. Wiley Encyclopedia of Biomedical Engineering, John Wiley & Sons, New York.
- Onik G, Mikus P, Rubinsky B. 2007. Irreversible electroporation: Implications for prostate ablation. *Technol Cancer Res Treat* 6(4):295–300.
- Pavlin M, Miklavčič D. 2003. Effective conductivity of a suspension of permeabilized cells: A theoretical analysis. *Biophys J* 85:719–729.
- Pavlin M, Miklavčič D. 2008. Theoretical and experimental analysis of conductivity, ion diffusion and molecular transport during cell electroporation—Relation between short-lived and long-lived pores. *Bioelectrochemistry* 74:38–46.

- Pavlin M, Pavšelj N, Miklavčič D. 2002. Dependence of induced transmembrane potential on cell density, arrangement, and cell position inside a cell system. *IEEE Trans Biomed Eng* 49:605–612.
- Pavlin M, Kandušer M, Reberšek M, Pucihar G, Hart FX, Magjarević R, Miklavčič D. 2005. Effect of cell electroporation on the conductivity of a cell suspension. *Biophys J* 88:4378–4390.
- Pavšelj N, Miklavčič D. 2008a. Numerical models of skin electropermeabilization taking into account conductivity changes and the presence of local transport regions. *IEEE Trans Plasma Sci* 36:1650–1658.
- Pavšelj N, Miklavčič D. 2008b. Numerical modeling in electroporation-based biomedical applications. *Radiol Oncol* 42:159–168.
- Pavšelj N, Bregar Z, Cukjati D, Batiuskaite D, Mir LM, Miklavčič D. 2005. The course of tissue permeabilization studied on a mathematical model of a subcutaneous tumor in small animals. *IEEE Trans Biomed Eng* 52:1373–1381.
- Pavšelj N, Préat V, Miklavčič D. 2007. A numerical model of skin electropermeabilization based on in vivo experiments. *Ann Biomed Eng* 35:2138–2144.
- Pliquett U. 2003. Joule heating during solid tissue electroporation. *Med Biol Eng Comput* 41(2):215–219.
- Pliquett U, Weaver JC. 1996. Electroporation of human skin: Simultaneous measurement of changes in the transport of two fluorescent molecules and in the passive electrical properties. *Bioelectrochem Bioenerg* 39(1):1–12.
- Prausnitz MR. 1999. A practical assessment of transdermal drug delivery by skin electroporation. *Adv Drug Deliv Rev* 35:61–76.
- Puc M, Kotnik T, Mir LM, Miklavčič D. 2003. Quantitative model of small molecules uptake after in vitro cell electropermeabilization. *Bioelectrochemistry* 60:1–10.
- Pucihar G, Mir LM, Miklavčič D. 2002. The effect of pulse repetition frequency on the uptake into electroporated cells in vitro with possible applications in electrochemotherapy. *Bioelectrochemistry* 57:167–172.
- Pucihar G, Kotnik T, Valič B, Miklavčič D. 2006. Numerical determination of transmembrane voltage induced on irregularly shaped cells. *Ann Biomed Eng* 34:642–652.
- Reilly JP. 1998. *Applied Bioelectricity, from Electrical Stimulation to Electropathology*, Springer-Verlag, New York.
- Rubinsky B, Onik G, Mikus P. 2007. Irreversible electroporation: A new ablation modality—Clinical implications. *Technol Cancer Res Treat* 6(1):37–48.
- Schoenbach KH, Beebe SJ, Buescher ES. 2001. Intracellular effect of ultrashort electrical pulses. *Bioelectromagnetics* 22:440–448.
- Šel D, Cukjati D, Batiuskaite D, Slivnik T, Mir LM, Miklavčič D. 2005. Sequential finite element model of tissue electropermeabilization. *IEEE Trans Biomed Eng* 52:816–827.
- Šel D, Maček-Lebar A, Miklavčič D. 2007. Feasibility of employing model-based optimization of pulse amplitude and electrode distance for effective tumor electroporated. *IEEE Trans Biomed Eng* 54:773–781.
- Šemrov D, Miklavčič D. 1998. Calculation of the electrical parameters in electrochemotherapy of solid tumors in mice. *Comput Biol Med* 28:439–448.
- Serša G, Jarm T, Kotnik T, Coer A, Podkrajšek M, Šentjurc M, Miklavčič D et al. 2008. Vascular disrupting action of electroporation and electrochemotherapy with bleomycin in murine sarcoma. *Br J Cancer* 98:388–398.
- Susil R, Šemrov D, Miklavčič D. 1998. Electric field induced transmembrane potential depends on cell density and organization. *Electro Magnetobiol* 17:391–399.
- Tekle E, Oubrahim H, Dzekunov SM, Kolb JF, Schoenbach KH, Chock PB. 2005. Selective field effects on intracellular vacuoles and vesicle membranes with nanosecond electric pulses. *Biophys J* 89:274–284.
- Towhidi L, Kotnik T, Pucihar G, Firoozabadi SMP, Mozdaran H, Miklavčič D. 2008. Variability of the minimal transmembrane voltage resulting in detectable membrane electroporation. *Electromagn Biol Med* 27:372–385.

- Tungjitusolmun S, Woo EJ, Cao H, Tsai J-Z, Vorperian VR, Webster JG. 2000. Thermal-electrical finite element modelling for radio frequency cardiac ablation: Effects of changes in myocardial properties. *Med Biol Eng Comput* 38:562–568.
- Valič B, Golzio M, Pavlin M, Schatz A, Faurie C, Gabriel B, Teissié J, Rols MP, Miklavčič D. 2003. Effect of electric field induced transmembrane potential on spheroidal cells: Theory and experiment. *Eur Biophys J* 32:519–528.
- Yamamoto T, Yamamoto Y. 1976a. Electrical properties of the epidermal stratum corneum. *Med Biol Eng* 14(2):151–158.
- Yamamoto T, Yamamoto Y. 1976b. Dielectric constant and resistivity of epidermal stratum corneum. *Med Biol Eng* 14(5):494–500.
- Županič A, Čorović S, Miklavčič D. 2008. Optimization of electrode position and electric pulse amplitude in electrochemotherapy. *Radiol Oncol* 42:93–101.